International Journal of Innovative
Computing, Information and Control
Volume 8, Number 11, November 2012
 ISSN 1349-4198
pp. 7501–7518

EXTRACTION AND SCREENING OF KNEE JOINT VIBROARTHROGRAPHIC SIGNALS USING THE INDEPENDENT COMPONENT ANALYSIS METHOD

Jien-Chen Chen[1], Pi-Cheng Tung[1,*], Shih-Fong Huang[2,3]
Shu-Wei Wu[1] and Shih-Lin Lin[4]

[1]Department of Mechanical Engineering
National Central University
No. 300, Jhongda Road, Jhongli City, Taoyuan County 32001, Taiwan
*Corresponding author: t331166@ncu.edu.tw

[2]Division of Nerve Repair
Department of Neurosurgery
Neurological Institute
Taipei Veterans General Hospital
No. 201, Sec. 2, Shipai Road, Beitou District, Taipei City 11217, Taiwan
shihfongh@yahoo.com

[3]School of Medicine
National Yang-Ming University
No. 155, Sec. 2, Linong Street, Taipei 11221, Taiwan

[4]China Engine Corporation
Taoyuan County, Taiwan

Received July 2011; revised November 2011

Abstract. *This study presents a novel method for the extraction and screening of knee joint vibroarthrographic (VAG) signals using an independent component analysis (ICA) technique. A time-frequency analysis technique of the extracted vibration signals is proposed to carry out knee joint diagnosis. The performance of the ICA technique is verified experimentally. Statistical pattern classification screening accuracy is 82.5% in VAG. The results confirm that ICA is a feasible approach for the noninvasive diagnosis and monitoring of articular cartilage pathology.*
Keywords: Vibroarthrographic, Independent component analysis

1. **Introduction.** The knee joint is the most commonly injured or diseased joint in the human body. Arthritic degeneration of an injured knee is a well-known phenomenon. Vibroarthrography, the recording of vibration or acoustic signals from the human knee joint during active movement of the leg, can be used as a noninvasive diagnostic tool to detect articular cartilage degeneration. Conventional imaging techniques and x-ray diagnostic tests are not feasible for accurate diagnosis of knee joint pathology because they are unable to show objective signs of degenerative joint disease, especially during early stages of deterioration. Even after gross cartilage degeneration or injury has occurred, changes cannot be detected in many cases without invasive tests such as arthroscopy [1-3]. Arthroscopy is one of the best-known diagnostic procedures for screening knee joint disorders. It is a semi invasive procedure wherein a fiber optic cable inserted into the knee joint allows the physician to look at the joint through an arthroscope. Due to the semi invasive nature, arthroscopy is not suitable for repeated assessment or follow-up studies for monitoring purposes. However, noninvasive imaging techniques such as X-rays and

computed tomography (CT) scans cannot detect knee joint disorders until they are in the advanced stages. Compared with the other imaging techniques, magnetic resonance imaging (MRI) is much more sensitive for knee joint disorders and is still evolving. MRI scanners are expensive and not commonly available, which make them an uneconomical choice, both in terms of money and time for screening purposes and particularly for follow-up studies [4-15].

The vibration signals emitted from knee joints during their flexion or extension provide valuable clues regarding their pathological condition or physiological state. As a result, vibroarthrography (VAG), specifically, the recording of human knee joint vibrations or acoustic signals during active movement of the leg, provides an invaluable noninvasive diagnostic tool for the early detection of articular cartilage degeneration. However, the detected joint signals can be contaminated with noise from a variety of sources, including the transducer used to detect the signal, the measurement apparatus, manual intervention during the test procedure, and so forth. Moreover, the resulting signal interference is not stable, but varies over time, from swing to swing and from one individual to another. Therefore, effective interference cancellation techniques are required to reduce the variability of the vibration signal so that more reliable diagnostic results can be obtained.

Early medical researchers had no choice but to use simple electric-stethoscopes or microphones for knee joint signal detection purposes. However, the signals detected using such instrumentation were inevitably afflicted with high levels of extraneous interference, arising from hand tremors, skin friction, background noise, and so forth. In 1976, Chu et al. [16] developed a double microphone differential amplifier setup to address this problem. However, while the proposed setup successfully suppressed extraneous background noise, it did not resolve the characteristic problem of all acoustic systems, namely a poor response to low-frequency signals (such as those generated in a knee joint) [17]. Modern VAG methods [6-12], in which the vibration signals are detected directly via accelerometers attached to the subject, are capable of measuring these lower frequency joint signals. However, the contact sensors used to detect the vibration signals are highly sensitive to low frequency inputs, and hence the VAG signal is severely contaminated by low-frequency artifacts caused by the muscle contraction required to move the knee for measurement purposes. This artifact, conventionally referred to as muscle contraction interference, encompasses all the signals induced by muscle contraction, including muscle activity, muscle sounds and tremors, vibromyographic signals, and so on [18]. A interference contribution of muscle contraction is inevitable in VAG applications, since the muscles involved in knee movement cannot be maintained in a totally relaxed state at all times during the measurement procedure, and the muscle contraction required to execute knee movement cannot be kept constant as the leg is swung backward and forward due to the inherent inertia of the movement.

Accordingly, in this paper, we propose an enhanced VAG detection and diagnosis method based on independent component analysis and time-frequency analysis, respectively. The proposed method is essentially an extension of that employed previously for the processing of the EEG signal produced by the neurons in the human brain [19].

ICA can be used to isolate the original independent sources in a set of mixed signals. Traditional VAG systems often received mixed signals from the VAG signal and other noises, causing difficulty in monitoring knee health. The use of ICA can improve the quality of VAG signals and ensure accurate understanding of the knee's condition. Other approaches of improving VAG quality have been tested in many studies [4-15]. However, none of these approaches is as simple and effective as ICA.

2. **Data Acquisition.** The experimental trials were carried using 23 subjects diagnosed with articular cartilage pathology and 12 subjects with no knee joint disability. As shown in Figure 1(a) and Figure 1(b), four miniature accelerometers (Model 353-B33, PCB Piezotronics Inc., USA) were attached to the subjects' skin using double-sided adhesive tape in regions of the knee corresponding to the lateral condyle of the femur (LCF), the medial condyle of the femur (MCF), the lateral condyle of the tibia (LCT), and the medial condyle of the tibia (MCT). The accelerometers were positioned such that the majority of the sensors detected the VAG signal, while the remainder monitored variations in the signal along the leg, providing information with which to discriminate the noise signals from the VAG signal. The resulting signals were amplified by a pre-amplifier (Model 482A20, PCB Piezotronics Inc., USA) and then output to an oscilloscope for observation purposes and a computer for data processing. The recorded signals were digitized with a sampling rate of 50k Hz, 24-Bit, using a signal data acquisition board (Model USB 9233, National Instruments Inc., USA) and processed using Labview software (National Instruments Inc., USA). Figure 1(b) shows an experimental trial for diagnosis of articular cartilage pathology.

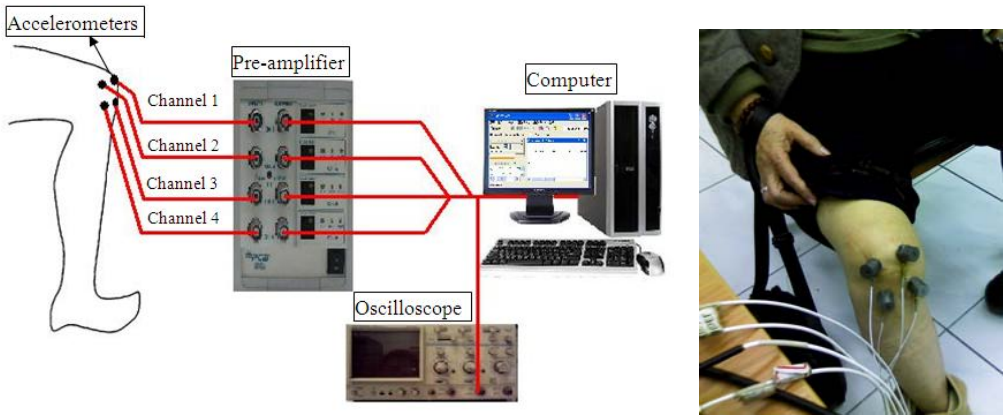

(a) (b)

FIGURE 1. (a) Schematic illustration of experimental setup, (b) experimental trial for diagnosis of articular cartilage degeneration

3. **VAG Signal Monitoring and Diagnosis Using ICA.** In the VAG scheme presented in this study, the signals obtained by the four accelerometers are processed using ICA to identify individual contributions of the VAG and noise signals. A time-frequency technique is then applied to further signal processing so that a reliable diagnostic result can be obtained. Figure 2 shows a block diagram of the overall VAG detection and diagnostic approach.

3.1. **Independent component analysis (ICA) theory.** In general, ICA is a method for separating a mutually-interfering mixture of signals in a multiple input system into a corresponding set of independent signals. In traditional VAG techniques, multiple sensors are applied to the patient's patella for detection of a mixture of signals from various sources, including muscle contraction signals, cartilage pathology signals, and various other noises originating from interior or exterior interference sources. ICA provides a powerful technique for separating these mixed signals so that each can be independently observed. ICA is a relatively new statistical technique and has been successfully applied for the processing of physiological signals [19-22].

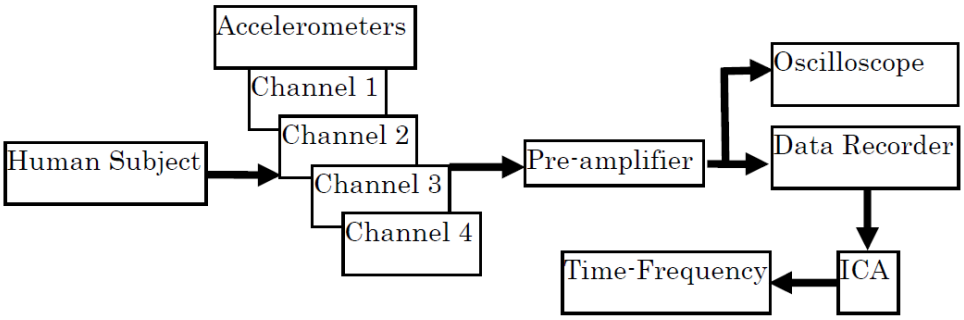

FIGURE 2. Block diagram of proposed detection and diagnosis technique

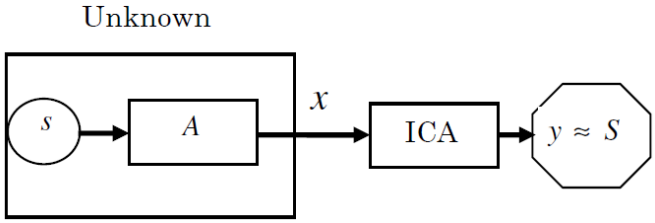

FIGURE 3. Schematic representation of independent component analysis

Figure 3 presents a block diagram representation of the ICA approach. In the ICA model, the observed data x are regarded as random variables in a single m-dimensional space. For convenience, the random variables can be expressed in the following matrix form:

$$x = As, \tag{1}$$

where A is a mixing matrix and $s = (s_1, s_2, \ldots, s_n)^T$ are the latent variables (i.e., the independent components). Generally speaking, ICA searches for a linear transformation of the form

$$y = wx, \tag{2}$$

where y denotes the estimated value of the independent components s, and w is an unmixing matrix. The aim is to render the $y = (y_1, y_2, \ldots, y_n)^T$ between the components as independently as possible. In other words, if the measured independent function $f(y_1, y_2, \ldots, y_n)$ is maximized, then $w = A^{-1}$. Thus, $y = (y_1, y_2, \ldots, y_n)^T$, which, processed by ICA, will be equal to the original latent variables, such as $s = (s_1, s_2, \ldots, s_n)^T$. The objective of ICA is to determine the linear transformation w of the dependent sensor signals x, which renders the outputs as independent; i.e., $y = wx$.

An appropriate linear transformation w can be identified by applying the following function approximation based on the maximum entropy principle [23]:

$$J(y) \propto [E\{G(y)\} - E\{G(v)\}]^2, \tag{3}$$

where E is the probability expectation; G denotes a non-quadratic function; and v is a Gaussian random variable. Here, $G(y) = (1/a_1) \log \cosh a_1 y$, where $1 < a_1 < 2$, and the mean of v is zero. The maximum entropy distribution for such variables is the Gaussian distribution. The changing factor is the Gaussian random variable of 1. G can be any non-quadratic function without restriction, for which the value will be zero when G is a quadratic function. The FastICA scheme identifies independent components by maximizing the negentropy [21]. According to Hyvärinen [23], the largest J values in $E\{G(w^T x)G(y)\}$ are attained at certain optima of $E\{G(w^T x)\}$. Nongaussianity is here

measured by the approximation of negentropy $J(w^T x)$ given in Equation (3). Under the delimitation of $E\{(w^T x)^2\} = \|w\|^2 = 1$, the optima of $E\{G(w^T x)\}$ are given by [23]

$$E\{xg(w^T x)\} - \beta w = 0, \tag{4}$$

where β is a constant that can be easily evaluated to give $\beta = E\{w_0^T xg(w_0^T x)\}$, where w_0 is the value of w at optimum and the function g is a derivative of G, similar to the analysis of Hyvärinen [24]. In this study, Equation (4) is solved using Newton's method, as described below. Denoting the function on the left-hand side of Equation (4) by F, Equation (4) can be expressed in terms of the partial differential of w; i.e.,

$$JF(w) = E\{xx^T g'(wx)\} - \beta I. \tag{5}$$

The objective of Newton's method in the current solution procedure is to identify the change in w following each iteration time-step in accordance with [27]

$$JF(w)\Delta w = -F(w). \tag{6}$$

Given some random variables, it is straightforward to linearly transform them into uncorrelated variables. Therefore, it would be tempting to try to estimate the independent components by such a method, which is typically called whitening. In terms of the covariance matrix, this obviously means that $E\{xx^T\} = I$, in which I is the unit matrix. Determining the extent of the modification in w for each time requires the computation of the inverse matrix of $JF(w)$. To simplify the calculation procedure, an approximation of the first term in Equation (6) is processed. After the data has been whitening, then

$$E\{xx^T g'(wx)\} \approx E\{xx^T\}E\{g'(wx)\} = E\{g'(w^T x)\}I. \tag{7}$$

Such an approximation is acceptable. The Jacobian matrix in Equation (5) can then be diagonalized as

$$JF(w) = [E\{g'(w^T x) - \beta\}]I. \tag{8}$$

Computing the inverse matrix is then fairly straightforward. Applying the approximation in Equation (8), the Newton iterative solution procedure will have the following form [25]:

$$\begin{aligned} w^+ &\triangleq w + \Delta w \\ &= w - [E\{xg'(w^T x) - \beta w\}]/[E\{g'(w^T x) - \beta\}] \\ w^* &\triangleq w^+ / \left\|w^+\right\|. \end{aligned} \tag{9}$$

This algorithm can be further simplified by multiplying both ends of Equation (9) by $\beta - E\{g'(w^T x)\}$. The resulting fixed-point iteration scheme then becomes

$$\begin{aligned} w &= E\{xg'(w^T x)\} - E\{g'(w^T x)\}w \\ w &= w^* / \left\|w^*\right\|. \end{aligned} \tag{10}$$

This was introduced in [26] using a more heuristic derivation. An earlier version (for kurtosis only) was derived as a fixed point iteration of a neural learning rule in [23], which is where its name comes from. The condition for convergence requires that the old vector w and the new vector w^+ be parallel, but not necessarily directed toward the same point. Since w and w^+ are parallel, convergence identifies the independent components, when the inner absolute value of both vectors is 1. FastICA uses Newton's method, a classical numerical analysis that optimizes the mixed matrix by the iteration of linear equations. It does not require learning rate as a parameter. This makes FastICA much more acceptable to the users. Moreover, VAG requires an algorithm with fast convergence speed. A. Hyvärinen [25] compared FastICA and a stochastic gradient employed in an information maximization approach, with the best learning rate sequence in a quasi-neural network.

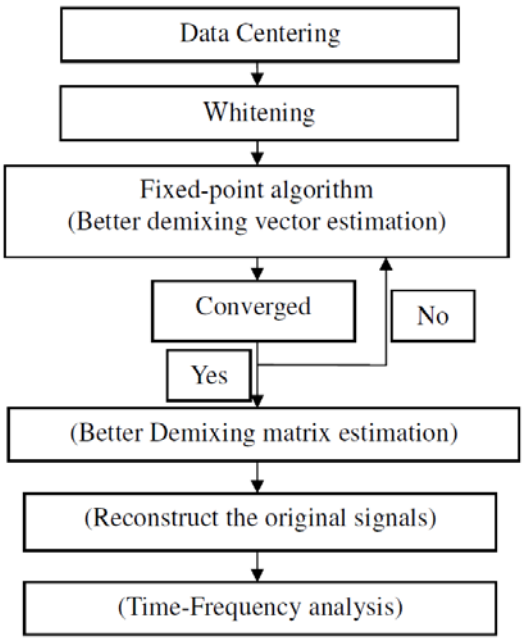

FIGURE 4. The whole computing flow of the ICA algorithm

The results showed that flops in FastICA are only 10% of the stochastic gradient. If the learning rate sequence was chosen in an trail-and-error manner without preliminary processing, the convergence speed of the fixed point algorithm would be 10^2 integer times faster than the series, and the stochastic gradient might not lead to convergence. Therefore, FastICA is more suitable for processing VAG signals. There are several conditions and constraints in the application of ICA to VAG. All the independent components s_i (i.e., VAG and noise interference) must be statistically independent, which means they must have the relation of $p(s_1, s_2, \ldots, s_i) = p_1(s_1)p_2(s_2)\ldots p_n(s_i)$. All the independent components s_i must have a non-Gaussian distribution. It is crucial to the efficacy of retrieving signals by ICA. However, according to the central limit theorem, one component is allowed to have a Gaussian distribution among grouped signals. The number of linear mixed signals $x_1(t)$ and $x_2(t)$ should be greater or equal to that of the independent components.

The computing steps proposed in this study are shown in Figure 4. The details of centering and whitening are mentioned in previous literature [21-25].

This study used a CPU-Core2 Duo 2.0GHz industrial computer with MATLAB R2007b software. The proposed approach of using ICA can improve the quality of VAG signals and ensure the accuracy of understanding the patient's knee condition. Other means of improving VAG quality have been tested in previous studies [4-15]. However, none of these means is as simple and effective as the proposed approach.

In ICA, the successful separation of the original signals is dependent on the fulfillment of the following conditions [24].

- The VAG are statistically independent from the knee signals.
- The number of sources is the same as the number of mixtures.
- There should be no (little) noise common to the sources and there should be no (minimal) delay between the signals of the different sources in the recordings.

3.2. **Hilbert transform (HT) theory.** The ICA approach described above allows isolation of the various signals detected by the accelerometers. The Hilbert transform is used

in the second stage of the proposed signal processing technique. The Hilbert transform $y(t)$ for an arbitrary signal $x(t)$ can be defined by [28]

$$y(t) = \frac{1}{\pi} p \int_{-\infty}^{+\infty} \frac{x(\tau)}{t-\tau} d\tau, \tag{11}$$

where p is the Cauchy principal value. In Equation (11), the Hilbert transform is defined as the convolution of the signal $x(t)$ with $1/t$. Therefore, the Hilbert transform is capable of identifying the local properties of $x(t)$. Coupling $x(t)$ and $y(t)$, we obtain the analytic signal $z(t)$ of $x(t)$

$$z(t) = x(t) + iy(t) = a(t)e^{i\theta(t)}, \tag{12}$$

where

$$a(t) = \sqrt{x^2(t) + y^2(t)}, \quad \theta(t) = \tan^{-1}\left(\frac{y(t)}{x(t)}\right). \tag{13}$$

The $a(t)$ is the instantaneous amplitude of $z(t)$, which can reflect how the energy of the $x(t)$ varies with time; and $\theta(t)$ is the instantaneous phase of $z(t)$. The controversial instantaneous frequency $\omega(t)$ is defined as the time derivative of the instantaneous phase $\theta(t)$, as follows:

$$\omega(t) = \frac{d\theta(t)}{dt}. \tag{14}$$

In the above process, both the amplitude and the instantaneous frequency are a function of time. This frequency-time distribution of the amplitude is designated as the Hilbert spectrum $H(\omega, t)$. After performing the Hilbert transform for the signal component, the original signal can be expressed as the real part, in the following form:

$$H(\omega, t) = \mathrm{Re} \sum_{i=1}^{n} a_i(t) e^{j \int \omega_i(t) dt}. \tag{15}$$

The Time-Frequency analysis technique is particularly suitable for characterizing signals at different localization levels over time and in different frequency domains. Then the marginal spectrum can be defined as [28]

$$h(\omega) = \int_0^T H(w, t) dt \tag{16}$$

where T is the total data length. The contribution of the total amplitude from each frequency is measured by the marginal spectrum.

4. **Experimental Study and Results.** The observed differences between normal and abnormal VAG signals are characterized using ICA and time-frequency analysis. The four VAG signals measured in the 10-second period for a subject with no knee disability are shown in Figure 5. Figures 5(a)-5(d) show mixed VAG and noise signals. The signals correspond to the gradual movement of the subject from a standing position to a squatting position and then back to an upright position over the 10-second interval. However, in the present form, these signals (shown in Figure 5) provide no insight into the pathological condition of the knee joint. Thus, they are transformed into a time-frequency figure by the Hilbert transform technique. This approach has the advantage that it can be easily constrained to yield the real distributions, which can be interpreted as a two-dimensional decomposition of a signal's energy. The resulting time-frequency analysis of the four signals illustrated in Figure 5 is presented in Figure 6. The temporal waveform of the VAG signal, which is a linear frequency modulation signal, and its instantaneous frequency, as calculated by Equations (14) and (15), are shown in this figure. The horizontal axis indicates the elapsed time, the vertical axis the frequency domain, and the color spectrum

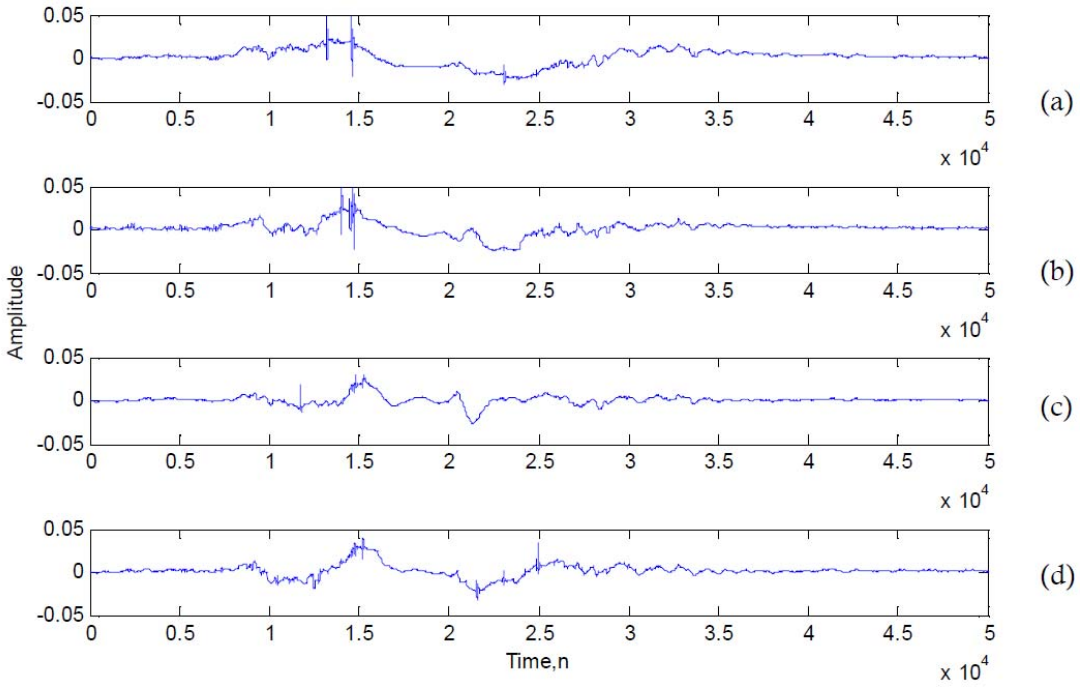

FIGURE 5. Signals acquired from healthy subject. (a) Medial condyle of femur (MCF), (b) lateral condyle of femur (LCF), (c) medial condyle of tibia (MCT), (d) lateral condyle of tibia (LCT).

the signal volume in dB. Low frequency signals that possess higher energy are presented in red, while high frequency signals are depicted in blue or green. The changes in the signals over time are clearly observable in the four sub-figures. The upper trace in Figure 6 indicates the time-frequency analysis of the VAG signals. The results show the high frequency signals processed by FastICA at 2-3 and 4-6 seconds. However, in the present form, these signals provide no insight into the pathological condition of the knee joint. Since the VAG and muscle contraction motion signals are of lower frequency, i.e., they are in the low frequency range, it is impossible to separate them using a classical filter. Furthermore, although the muscle contraction interference signals can be canceled using an adaptive filter, the noise signal continues to interfere with the VAG signal. Therefore, in the signal processing scheme developed in this study, FastICA is used to identify the mixed matrix w and to reconstruct the four VAG signals. An X-Ray image of degenerative knee joint pathology is shown in Figure 7. Figure 8 shows the accelerometer-detected signals for a subject known to have degenerative knee joint pathology. The VAG signals from the subject with degenerative knee joint pathology and processed by FastICA are shown in Figure 9. The time-frequency of the signals given in expression (14) and (15) is illustrated by the contour in Figure 10. As can be seen in Figure 10, the range between the high energy and the low energy is about 250 Hz. High-energy signals on the VAG signal band occur at 1-6 seconds. In contrast, the VAG and noise signals can be clearly identified. The VAG signal is seen to have duration of approximately 1-6 seconds. The upper trace shows the VAG signal, while the other three traces indicate the noise signals. The standing and squatting positions can be observed as one period beat of 10 seconds. The loading of the joint and the friction are indicated by the higher energy of the VAG signals. This higher energy confirms the degenerative knee joint pathology. The frequency changes in the signals are clearly observable. One obvious visual difference between normal and abnormal signals is that the amplitude of the variability between the

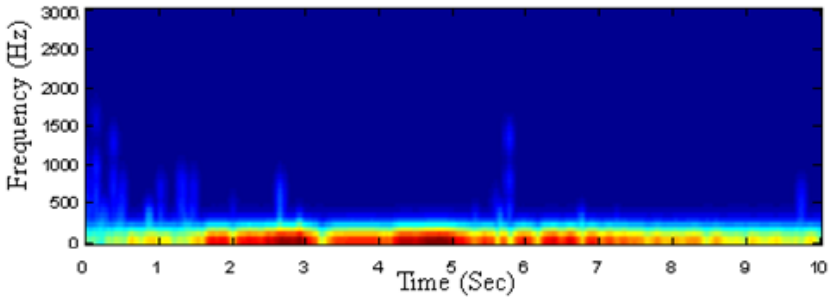

(a) Medial condyle of femur (MCF)

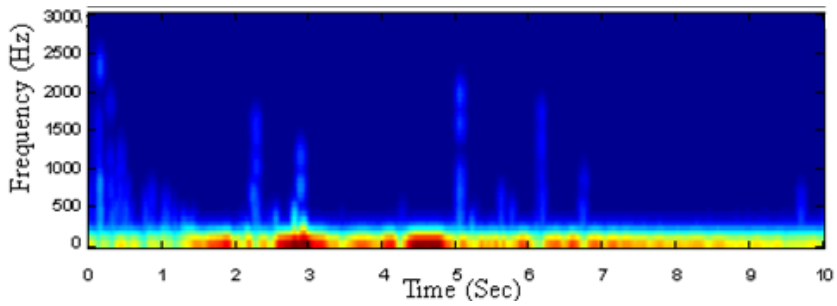

(b) Lateral condyle of femur (LCF)

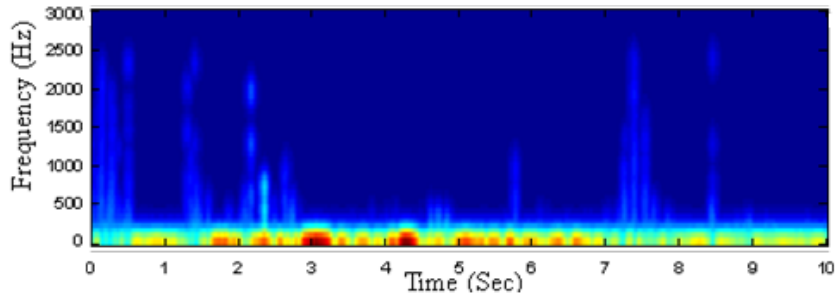

(c) Medial condyle of tibia (MCT)

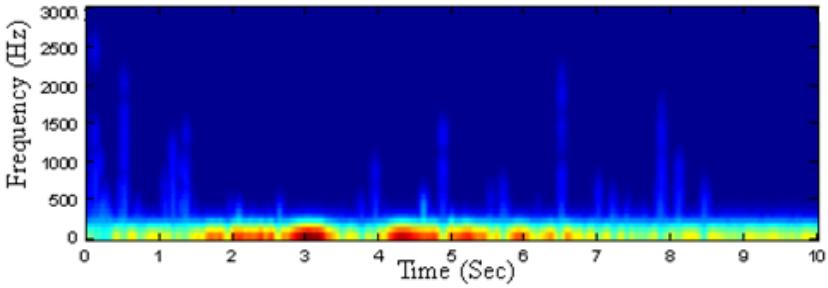

(d) Lateral condyle of tibia (LCT)

FIGURE 6. Time-frequency analysis of VAG signals acquired from healthy subject

standing and squatting ends of the cycle is much greater for abnormal signals than for normal signals. Visual comparison indicates that the time-frequency result has preserved most of the important characteristics, especially the transient component. Figure 11(I) to Figure 11(XII), which show practical examples of 12 subjects with articular cartilage degeneration, respectively. The abnormal signals shown in Figure 11(b) are higher in value than the normal signals shown in Figure 6, confirming the expectation that the VAG signal conveys more discriminatory information during extension than flexion, due to increased loading of the knee joint during the standing and squatting movement of the leg. The proposed approach in the paper uses ICA to isolate the original independent

FIGURE 7. X-ray image of an abnormal knee

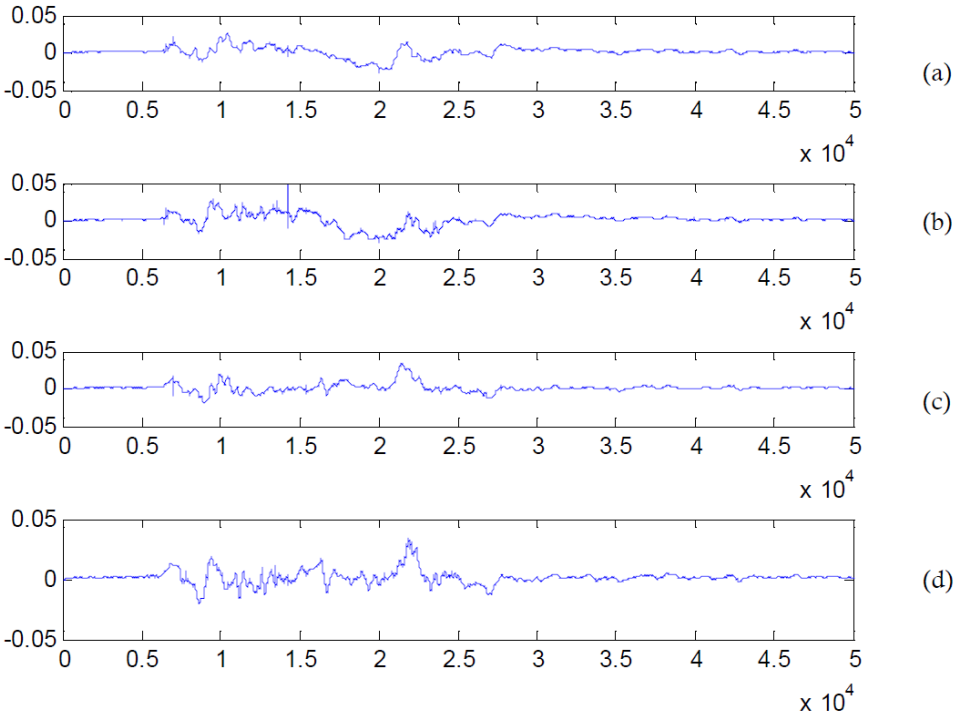

FIGURE 8. VAG signals from subject with degenerative knee joint pathology. (a) Medial condyle of femur (MCF), (b) lateral condyle of femur (LCF), (c) medial condyle of tibia (MCT), (d) lateral condyle of tibia (LCT).

sources in a set of mixed signals. Traditional VAG systems often receive mixed signals from other noises, causing difficulty in diagnosis. The use of ICA can improve the quality of VAG signals and ensure the accuracy of understanding the patient's condition. However, imaging-based noninvasive techniques such as X-rays can capture only gross cartilage defects, and may not be useful for early detection of articular cartilage degeneration. The proposed approach in this paper utilizes a simple instrument to diagnose and monitor articular cartilage degeneration for patients at any time. As can be seen in Figure 11(b), the range between the high energy and the low energy is about 250 Hz. High-energy signals on the VAG signal band occur at 2-8 seconds. However, there are some limitations to this approach. First, during the diagnosis, the patient needs to move from a standing position to a squatting position and then return to an upright position over the 10-second interval. In serious cases, the patient will be unable to do the test. Secondly, experienced experts must diagnose articular cartilage degeneration from the time-frequency diagram. It is crucial to the efficacy of retrieving signals by ICA. We hope an extraction system may be developed to perform auto-diagnosis based on the measured VAG signals. The

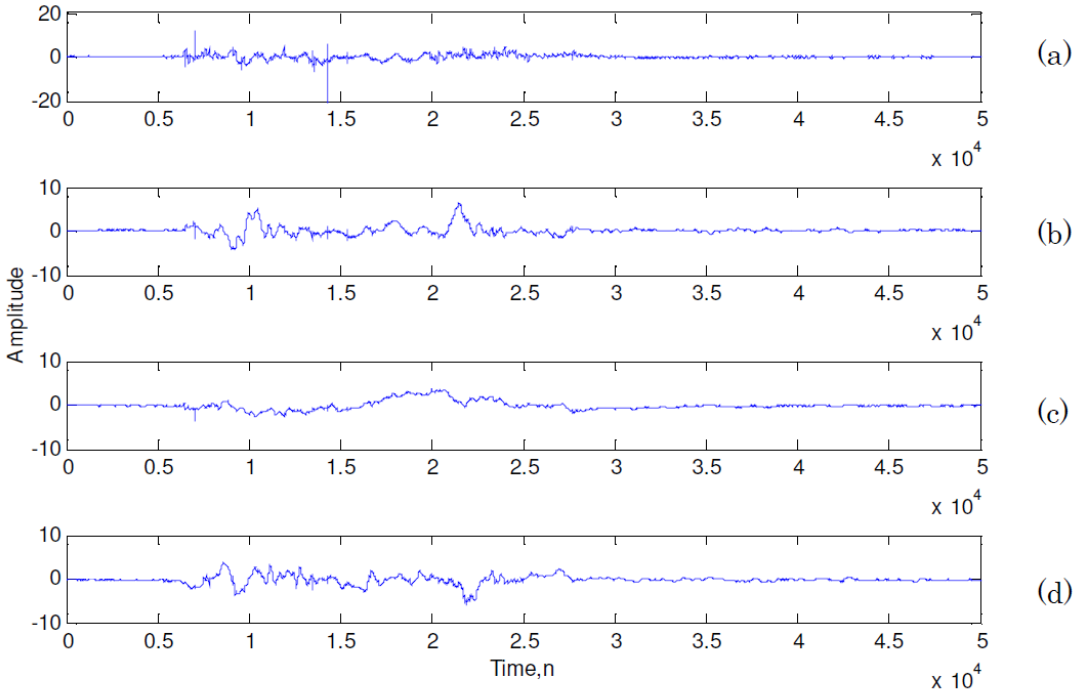

FIGURE 9. VAG signals from subject with degenerative knee joint pathology processed by FastICA. (a) Medial condyle of femur (MCF), (b) lateral condyle of femur (LCF), (c) medial condyle of tibia (MCT), (d) lateral condyle of tibia (LCT).

TABLE 1. R.M.S of the proposed features for normal VAG signals

Normal signals	MCF RMS($m/\sec^2$)	LCF RMS($m/\sec^2$)	MCT RMS($m/\sec^2$)	LCT RMS($m/\sec^2$)
1	0.0074	0.0094	0.0089	0.0127
2	0.0087	0.0068	0.0070	0.0065
3	0.0042	0.0084	0.0044	0.0099
4	0.0082	0.0076	0.0053	0.0052
5	0.0070	0.0082	0.0084	0.0103
6	0.0090	0.0074	0.0054	0.0057
7	0.0092	0.0077	0.0053	0.0074
8	0.0053	0.0073	0.0044	0.0047
9	0.0049	0.0057	0.0057	0.0073
10	0.0079	0.0076	0.0039	0.0059
11	0.0061	0.0055	0.0063	0.0063
12	0.0117	0.0073	0.0097	0.0106
mean	0.0075	0.0074	0.0062	0.0079
SD	0.0020	0.0010	0.0018	0.0024

improvement in signal detection technique is a significant contribution to the analysis of VAG signals even though the measured VAG signals are in a low signal-to-noise (NSR) situation.

Table 1 shows the root mean square (RMS) of the proposed features for the normal VAG signals. Table 2 shows the RMS of the proposed features for the abnormal VAG

signals. The mean and standard deviation (SD) of the classification performance are recorded in Table 1 and Table 2. The mean and SD of knee acceleration signals in the range of 100-500 Hz are found to be significantly different for abnormal (with degenerative knee joint pathology) compared with normal (without degenerative knee joint pathology) signals. The abnormal signals are higher in value, confirming the expectation that the VAG signal conveys more discriminatory information during extension than flexion, due

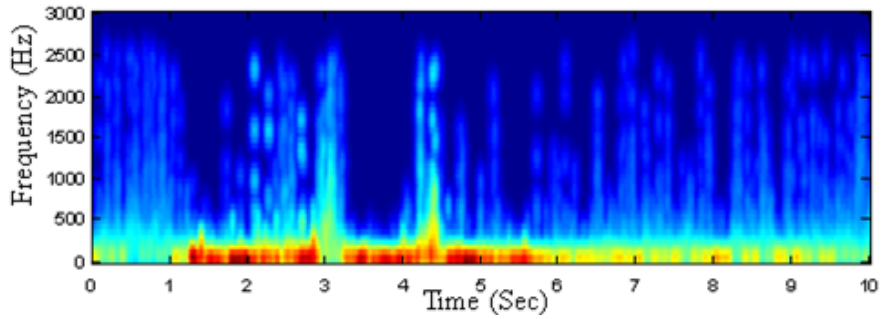

(a) Medial condyle of femur (MCF)

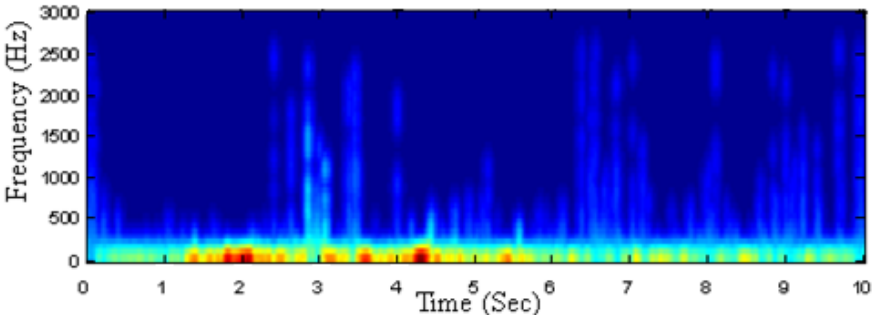

(b) Lateral condyle of femur (LCF)

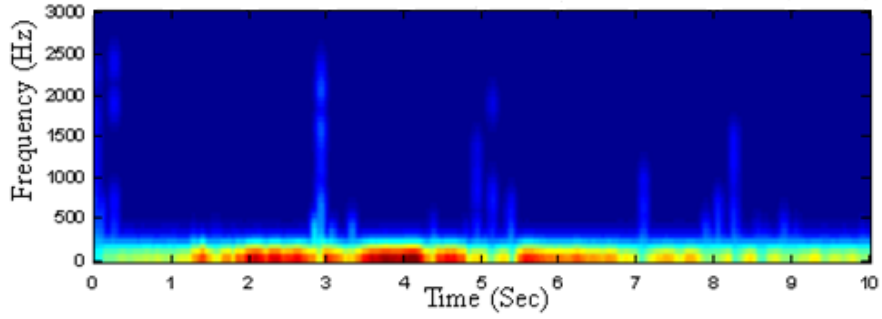

(c) Medial condyle of tibia (MCT)

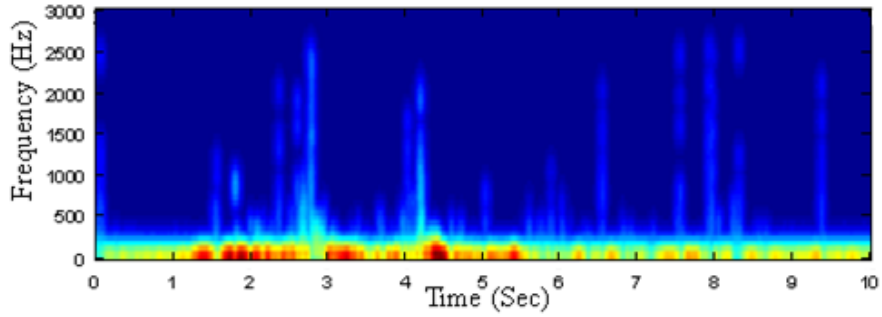

(d) Lateral condyle of tibia (LCT)

FIGURE 10. Time-frequency analysis of VAG signals in Figure 9

I

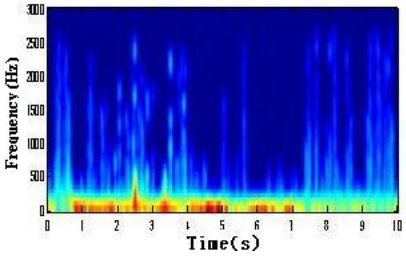

I

II

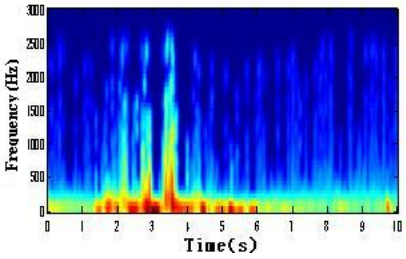

II

III

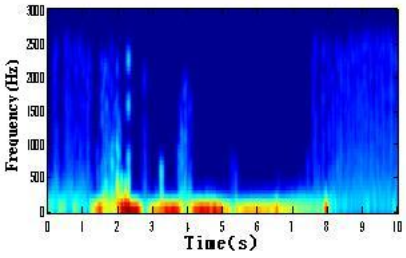

III

IV

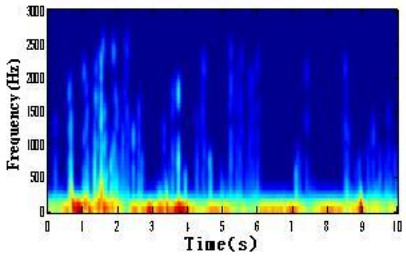

IV

V

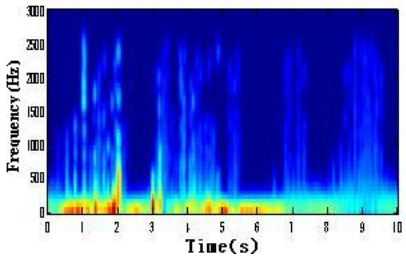

V

VI

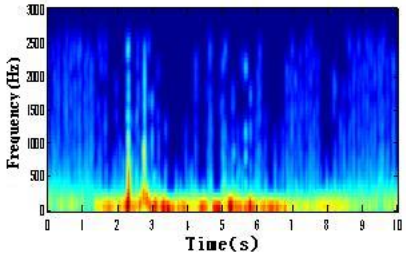

VI

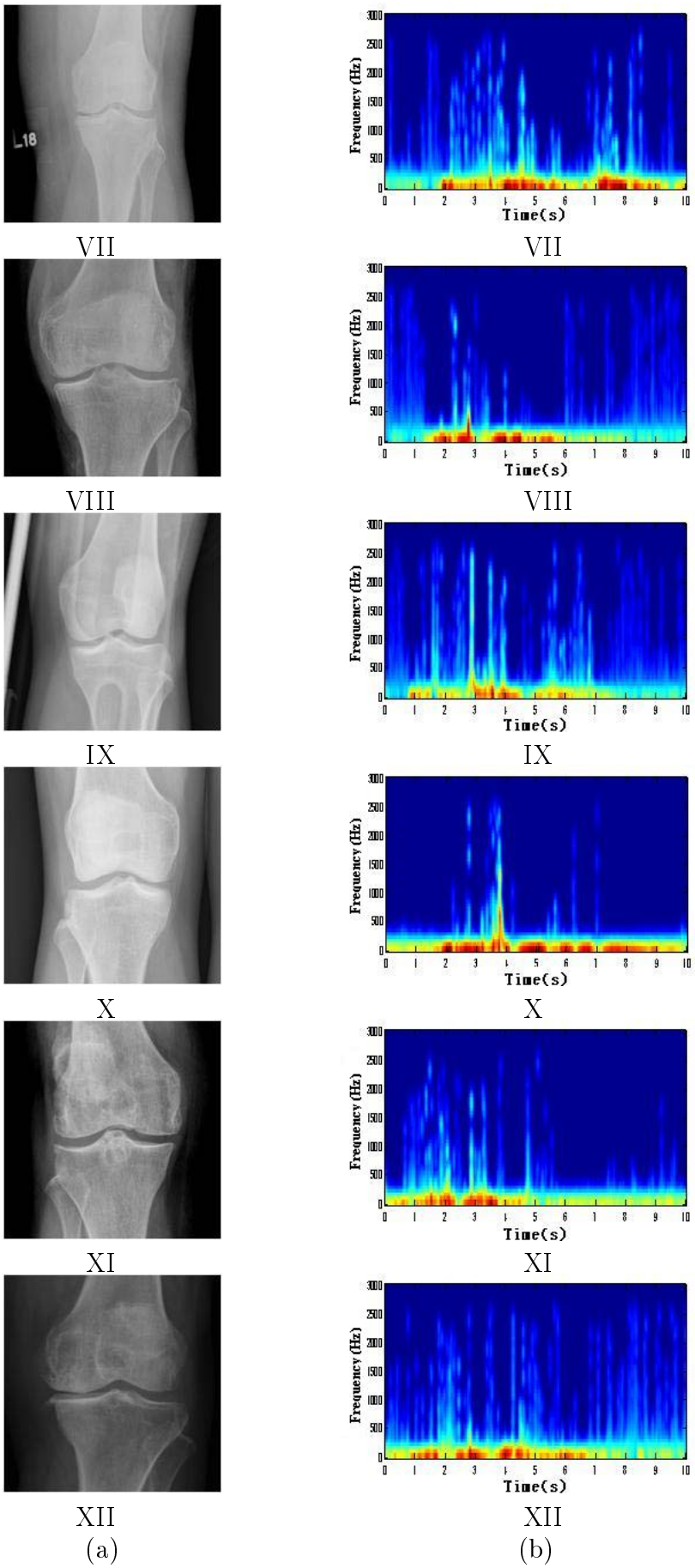

FIGURE 11. (a) X-ray image of abnormal knee, (b) time-frequency analysis of VAG signals

TABLE 2. R.M.S of the proposed features for abnormal VAG signals

Abnormal signals	MCF RMS($m/\sec^2$)	LCF RMS($m/\sec^2$)	MCT RMS($m/\sec^2$)	LCT RMS($m/\sec^2$)
1	1.0107	0.9948	0.9998	0.9998
2	1.0107	0.9984	0.9961	1.0000
3	0.9950	0.9994	0.9994	0.9998
4	0.9853	1.0000	1.0000	1.0001
5	1.0005	0.9968	1.0014	1.0000
6	1.0759	0.9973	1.0002	0.9995
7	0.9994	0.9979	1.0000	0.9998
8	1.0001	1.0001	1.0003	0.9998
9	0.9579	1.0001	0.9999	0.9999
10	0.9994	1.0004	0.9996	0.9990
11	0.9980	0.9988	0.9996	0.9998
12	0.9996	1.0022	1.0000	1.0005
13	0.9928	0.9965	0.9985	0.9999
14	0.9985	0.9997	1.0129	1.0005
15	1.0004	1.0000	0.9987	0.9997
16	1.0024	1.0003	1.0003	1.0004
17	0.9968	0.9944	0.9998	1.0005
18	1.0011	1.0004	1.0000	1.0009
19	0.9838	1.0001	1.0003	1.0006
20	1.0010	0.9992	0.9994	1.0006
21	1.0003	0.9997	0.9990	1.0004
22	0.9898	1.0002	0.9998	1.0000
23	1.0009	1.0005	1.0044	1.0000
mean	1.0000	0.9990	1.0004	1.0000
SD	0.0192	0.0019	0.0030	0.00042

to increased loading of the knee joint during the standing and squatting movement of the leg.

In comparison with the results reported in previous studies [2,30-32] on the analysis of VAG signals, the results obtained in the present study are important. The proposed parameters, derived from the VAG signals with no segmentation and no additional clinical information, have provided screening accuracies comparable to or better than those obtained with more sophisticated methods [2,30-32]. Krishnan et al. [2], who used the matching pursuit time-frequency distribution (TFD), a nonstationary signal analysis tool, to avoid segmentation and joint angle estimation. The best normal versus abnormal classification accuracy achieved was 68.9% as evaluated by TFD. Rangayyan et al. [30] derived dominant poles and cepstral coefficients using logistic regression analysis from CC-LRA models of adaptively segmented VAG signals using the same database as above. The cepstral coefficients appeared to be the best discriminant features, providing a classification accuracy of 75.6%, as evaluated by CC-LRA. Krishnan et al. [31] derived autoregressive (AR) coefficients from VAG signal segments and tested the methods with a database of VAG signals of 90 subjects (51 normal subjects and 39 abnormal subjects); the methods provided a classification accuracy of 68.9% using logistic regression analysis (AR-LRA).

TABLE 3. Comparison of the classification accuracies using different feature extraction and pattern classification methods [29]

Method	Subject number	Diagnosed results		Average accuracy (%)
		Normal	Abnormal	
TFD [2]	Normal (51)	40	11	
	Abnormal (39)	17	22	68.9
CC-LRA [30]	Normal (51)	N/A	N/A	
	Abnormal (39)	N/A	N/A	75.6
AR-LRA [31]	Normal (51)	N/A	N/A	
	Abnormal (39)	N/A	N/A	68.9
WD-LDA [32]	Normal (51)	38	13	
	Abnormal (38)	8	30	76.4
The proposed ICA	Normal (12)	10	2	
	Abnormal (23)	3	20	82.5

Recently, Umapathy and Krishnan [32] applied wavelet packet decomposition and a modified local discriminant based algorithm (WD-LDA) to the 89 VAG signals as in the present work (51 normal subjects and 38 abnormal subjects), and achieved a classification accuracy of 76.4% using linear discriminant analysis (WD-LDA). Table 3 shows the comparison of the classification accuracy using different feature extraction and pattern classification methods. We compare the other classification accuracies and the ICA method. The proposed approach provides a classification accuracy of 82.5%. The results confirm that the proposed scheme can successfully separate mixed signals, thereby enabling medical staff to better monitor degenerative knee joints.

The results confirm that the FastICA scheme can successfully separate mixed signals, thereby enabling medical staff to better monitor degenerative knee joint pathology.

5. **Discussion.** A novel approach to illuminating noise from VAG signals so as to enhance feature extraction and identify problems is proposed. Since VAG applications require the use of algorithms with a rapid convergence speed, FastICA is more suitable for processing VAG signals. The ICA and time-frequency analysis scheme presented in this study makes a significant contribution to the detection and diagnosis of VAG signals and is intended to pave the way toward the development of an enhanced non-invasive technique for monitoring knee joint heath.

Further detailed studies of knee joint disorder monitoring must be carried out with a large number of patients. We are also conducting further investigations of more advanced methods for feature selection, nonlinear pattern classification, and the optimization of the parameters of the classifier.

Acknowledgments. The work is supported in part by the National Science Council in Taiwan, under contract No. NSC 100-2221-E-008-031-MY2.

REFERENCES

[1] C. B. Frank, R. M. Rangayyan and G. D. Bell, Analysis of knee joint sound signals for non-invasive diagnosis of cartilage pathology, *IEEE Eng. in Medicine and Biology Magazine*, pp.65-68, 1990.

[2] S. Krishnan, R. M. Rangayyan, G. D. Bell and C. B. Frank, Adaptive time-frequency analysis of knee joint vibroarthrographic signals for noninvasive screening of articular cartilage pathology, *IEEE Trans. Biomed. Eng.*, vol.47, no.6, pp.773-783, 2000.

[3] C. Jiang, J. Lee and T. Yuan, Vibration arthrometry in patients with failed total knee replacement, *IEEE Trans. Biomed. Eng.*, vol.47, no.2, pp.219-227, 2000.

[4] M. L. Chu, I. A. Gradisar, M. R. Railey and G. F. Bowling, An electroacoustical technique for the detection of knee joint noise, *Medical Research Engineering*, vol.12, no.1, pp.18-20, 1976.

[5] R. A. B. Mollan, G. C. McCullagh and R. I. Wilson, A critical appraisal of auscultation of human joints, *Clinical Orthopaedics and Related Research*, vol.170, pp.231-237, 1982.

[6] Y. T. Zhang, C. B. Frank, R. M. Rangayyan and G. D. Bell, Mathematical modeling and spectral analysis of the patella-femoral pulse train produced during slow knee movement, *IEEE Trans. Biomed. Eng.*, vol.39, no.9, pp.971-979, 1992.

[7] Y. T. Zhang, K. O. Ladly, R. M. Rangayyan, C. B. Frank, G. D. Bell and Z. Q. Liu, Muscle contraction interference in acceleration vibroarthrography, *Proc. of the IEEE/EMBS 12th Annual International Conference*, pp.2150-2151, 1990.

[8] Y. T. Zhang, R. M. Rangayyan, C. B. Frank and G. D. Bell, Adaptive cancellation of muscle contraction interference from knee joint vibration signals, *IEEE Trans. Biomed. Eng.*, vol.41, no.2, pp.181-191, 1994.

[9] S. Krishnan, R. M. Rangayyan, G. D. Bell and C. B. Frank, Sonification of knee-joint vibration signals, *Proc. of the 22nd IEEE Annu. Int. Conf. IEEE Engineering in Medicine and Biology Society*, pp.1995-1998, 2000.

[10] Y. Shen, R. M. Rangayyan, G. D. Bell, C. B. Frank, Y. T. Zhang and K. O. Ladly, Localization of knee joint cartilage pathology by multichannel vibroarthrography, *Medical Engineering & Physics*, vol.17, pp.583-594, 1995.

[11] S. C. Huang, I. P. Wei, H. L. Chien, T. M. Wang, Y. H. Liu, H. L. Chen, T. W. Lu and J. G. Lin, Effects of severity of degeneration on gait patterns in patients with medial knee osteoarthritis, *Medical Engineering & Physics*, vol.30, pp.997-1003, 2008.

[12] G. Spahn, H. Plettenberg, H. Nagel, E. Kahl, H. M. Klinger, T. Mückley, M. Günther, G. O. Hofmann and J. A. Mollenhauer, Evaluation of cartilage defects with near-infrared spectroscopy (NIR): An ex vivo study, *Medical Engineering & Physic*, vol.30, pp.285-292, 2008.

[13] P. Julkunen, R. K. Korhonen, W. Herzog and J. S. Jurvelin, Uncertainties in indentation testing of articular cartilage: A fibril-reinforced poroviscoelastic study, *Medical Engineering & Physics*, vol.30, pp.506-515, 2008.

[14] C. Provatidis, C. Vossou, E. Petropoulou, A. Balanika and G. Lyritis, A finite element analysis of a T12 vertebra in two consecutive examinations to evaluate the progress of osteoporosis, *Medical Engineering & Physics*, vol.31, no.6, pp.632-641, 2009.

[15] J. R. Steele, A. Basu and A. Job, A three-dimensional representation of an athletic female knee joint using magnetic resonance imaging, *Medical Engineering & Physics*, vol.16, pp.363-369, 1994.

[16] M. L. Chu, I. A. Gradisar, M. R. Railey and G. F. Bowling, An electro acoustical technique for the detection of knee joint noise, *Medical Research Engineering*, vol.12, no.1, pp.18-20, 1976.

[17] R. A. B. Mollan, W. G. Kemohan and P. H. Watters, Artefact encountered by the vibration detection system, *J. Biomechanics*, vol.16, no.3, pp.193-199, 1983.

[18] C. Orizio, R. Perini, B. Diemont, M. M. Figini and A. Veicsteinas, Spectral analysis of muscular sound during isometric contraction of biceps, *Journal of Applied Physiology*, vol.68, no.2, pp.508-512, 1990.

[19] S. Makeig, M. Westerfield, T. P. Jung, S. Enghoff, J. Townsend, E. Courchesne and T. J. Sejnowski, Dynamic brain sources of visual evoked responses, *Science*, vol.295, pp.690-694, 2002.

[20] H. Stögbauer, A. Kraskov, S. A. Astakhov and P. Grassberger, Least dependent component analysis based on mutual information, *Phys. Rev. E.*, vol.70, no.066123, 2004.

[21] T. W. Lee, *Independent Component Analysis: Theory and Applications*, Kluwer Academic Publishers, Boston, 1998.

[22] T. Tateyama, Z. Nakao, X. Han and Y.-W. Chen, Contrast enhancement of mr brain images by canonical correlations based kernel independent component analysis, *International Journal of Innovative Computing, Information and Control*, vol.5, no.7, pp.1857-1866, 2009.

[23] A. Hyvärinen and E. Oja, A fast fixed-point algorithm for independent component analysis, *Neural Computation*, vol.9, no.7, pp.1483-1492, 1997.

[24] A. Hyvärinen, Complexity pursuit: Separating interesting components from time-series, *Neural Computation*, vol.13, no.4, pp.883-898, 2001.

[25] A. Hyvärinen, Fast and robust fixed-point algorithms for independent component analysis, *IEEE Transactions on Neural Networks*, vol.10, no.3, pp.626-634, 1999.

[26] A. Hyvärinen, A family of fixed-point algorithms for independent component analysis, *Proc. of IEEE Int. Conf. Acoust., Speech Signal Processing*, Munich, Germany, pp.3917-3920, 1997.

[27] A. Hyvärinen and E. Oja, Independent component analysis: Algorithms and applications, *Neural Networks*, vol.13, no.4-5, pp.411-430, 2000.

[28] N. E. Huang, Z. Shen, S. R. Long, M. Wu, H. Shih, N. Zheng, C. Yen, C. C. Tung and H. H. Liu, The empirical mode decomposition and the Hilbert spectrum for non-linear and non-stationary time series analysis, *Proc. of the Royal Society of London Series A – Mathematical Physical and Engineering Sciences*, vol.454, pp.903-995, 1998.

[29] T. Mu, A. K. Nandi and R. M. Rangayyan, Screening of knee-joint vibroarthrographic signals using the strict 2-surface proximal classifier and genetic algorithm, *Computers in Biology and Medicine*, vol.38, pp.1103-1111, 2008.

[30] R. M. Rangayyan, S. Krishnan, G. D. Bell, C. B. Frank and K. O. Ladly, Parametric representation and screening of knee joint vibroarthrographic signals, *IEEE Trans. Biomed. Eng.*, vol.44, pp.1068-1074, 1997.

[31] S. Krishnan, R. M. Rangayyan, G. D. Bell, C. B. Frank and K. O. Ladly, Adaptive filtering, modelling and classification of knee joint vibroarthrographic signals for non-invasive diagnosis of articular cartilage pathology, *Med. Biol. Eng. Comput.*, vol.35, pp.677-684, 1997.

[32] K. Umapathy and S. Krishnan, Modified local discriminant bases algorithm and its application in analysis of human knee joint vibration signals, *IEEE Trans. Biomed. Eng.*, vol.53, pp.517-523, 2006.